Published in final edited form as:
J Neurosci. 2012 June 13; 32(24): 8254–8262. doi:10.1523/JNEUROSCI.0305-12.2012.

Gender Modulates the *APOE* ε4 Effect in Healthy Older Adults: Convergent Evidence from Functional Brain Connectivity and Spinal Fluid Tau Levels

Jessica S. Damoiseaux[1], **William W. Seeley**[2], **Juan Zhou**[3], **William R. Shirer**[1], **Giovanni Coppola**[4], **Anna Karydas**[2], **Howard J. Rosen**[2], **Bruce L. Miller**[2], **Joel H. Kramer**[2], **Michael D. Greicius**[1], and **Alzheimer's Disease Neuroimaging Initiative (ADNI)**[†]

[1]Functional Imaging in Neuropsychiatric Disorders (FIND) Lab, Department of Neurology and Neurological Sciences, Stanford University School of Medicine, Stanford

[2]Memory and Aging Center, Department of Neurology, University of California San Francisco

[3]Neuroscience and Behavioral Disorders Program, Duke-NUS Graduate Medical School, Singapore

[4]Semel Institute for Neuroscience and Human Behavior, Departments of Psychiatry & Neurology, David Geffen School of Medicine, University of California, Los Angeles

Abstract

We examined whether the effect of *APOE* genotype on functional brain connectivity is modulated by gender in healthy older human adults. Our results confirm significantly decreased connectivity in the default mode network in healthy older *APOE* ε4 carriers compared to ε3 homozygotes. More importantly, further testing revealed a significant interaction between *APOE* genotype and gender in the precuneus, a major default mode hub. Female ε4 carriers showed significantly reduced default mode connectivity compared to either female ε3 homozygotes or male ε4 carriers, whereas male ε4 carriers differed minimally from male ε3 homozygotes. An additional analysis in an independent sample of healthy elderly using an independent marker of Alzheimer's disease, i.e. spinal fluid levels of tau, provided corresponding evidence for this gender by *APOE* interaction. Taken together, these results converge with previous work showing a higher prevalence of the ε4 allele among women with Alzheimer's disease and, critically, demonstrate that this interaction between *APOE* genotype and gender is detectable in the preclinical period.

Introduction

The most important known risk factor for Alzheimer's disease (AD) is the presence of the Apolipoprotein E type 4 allele (*APOE* ε4) (Strittmatter et al., 1993). Carriers of the *ε4* allele have an increased risk of developing AD compared to people that are homozygous for the *ε3*

Corresponding author 1: Jessica S. Damoiseaux, PhD, Functional Imaging in Neuropsychiatric Disorders Lab, Department of Neurology and Neurological Sciences, Stanford University School of Medicine, 780 Welch Road, Suite 105, Palo Alto, CA 94304, T: (650) 721.6136, F: (650) 724.4432, jeske@stanford.edu; Corresponding author 2: Michael D Greicius, MD, Functional Imaging in Neuropsychiatric Disorders Lab, Department of Neurology and Neurological Sciences, Stanford University School of Medicine, 780 Welch Road, Suite 201, Palo Alto, CA 94304, T: (650) 498.4624, F: (650) 724.4432, greicius@stanford.edu.

[†]The cerebrospinal data used in the preparation of this article were obtained from the Alzheimer's Disease Neuroimaging Initiative (ADNI) database (www.loni.ucla.edu/ADNI). As such, the investigators within the ADNI contributed to the design and implementation of ADNI and/or provided data but did not participate in analysis or writing of this report. A complete listing of ADNI investigators can be found at: http://adni.loni.ucla.edu/wp-content/uploads/how_to_apply/ADNI_Acknowledgement_List.pdf

Supplementary materials: None

Conflict of Interest: None

allele (the most common *APOE* genotype) (Farrer et al., 1997). An important observation that tends to be overlooked is that this *APOE* effect varies with gender. Women are more likely to develop AD than men across most ages and *APOE* genotypes (Farrer et al., 1997), but this difference is significantly more pronounced in people with the *APOE* ε3/ε4 genotype, where women increase their risk approximately four-fold and men show little to no increased risk (Payami et al., 1996; Farrer et al., 1997; Bretsky et al., 1999). In addition to having an increased risk for developing AD, female *ε4* carriers with mild cognitive impairment (MCI), a precursor to AD, also express more prominent phenotypic features than their male counterparts; for example, lower hippocampal volumes and worse cognitive scores (Fleisher et al., 2005). A large autopsy series found that female ε4 carriers also had the greatest amyloid plaque and neurofibrillary tangle pathology (Corder et al., 2004). To date, this interaction between gender and *APOE* status, evident in AD risk, MCI phenotypes, and post-mortem data, has not been explored in-vivo in healthy older subjects.

Previous resting state functional magnetic resonance imaging (fMRI) studies have shown functional connectivity changes in the default mode network (DMN) in MCI (Sorg et al., 2007)) and AD (Greicius et al., 2004; Wang et al., 2007; Zhang et al., 2009), and that this default mode functional connectivity deteriorates as the disease progresses (Bai et al., 2011; Damoiseaux et al., 2011). Recent resting state fMRI studies have investigated whether we can detect similar changes in brain functional connectivity in healthy older *ε4* carriers (Sheline et al., 2010; Machulda et al., 2011; Trachtenberg et al., 2011; Westlye et al., 2011). Trachtenberg and colleagues found no *APOE*-related differences in DMN connectivity. The other three studies show significant DMN connectivity differences between ε4 carriers and ε3 homozygotes, although there is substantial variability in their results. None of these studies examined whether the observed default mode functional connectivity differences varied by gender. In this study we examined the effect of *APOE* genotype and gender on default mode functional connectivity in healthy older subjects. In line with previous research, we expected to see a pattern similar to what we have observed in AD, that is, decreased connectivity in the DMN (Greicius et al., 2004; Damoiseaux et al., 2011), with the greatest effect in female *ε4* carriers. In order to obtain convergent evidence for these imaging findings we also tested the same model in an analysis of spinal fluid protein levels in healthy older controls from the Alzheimer's Disease Neuroimaging Initiative (ADNI) dataset.

Materials and Methods

Participants in the UCSF/Stanford Study

Healthy older adults were recruited as part of longitudinal study of normal aging at the University of California, San Francisco (UCSF). All participants provided informed consent according to the Declaration of Helsinki and the Institutional Review Board at UCSF approved the procedures. Exclusion criteria for this study were the following: left-handedness; any significant medical, neurological or psychiatric illness; a history of brain damage; use of psychoactive medication; poor data quality; and carrying an *ε2* allele. *APOE* ε2 may have a protective effect against developing AD (Scott et al., 1997), therefore we have excluded these subjects from our analyses. Resting state fMRI data and *APOE* genotype were available for 234 participants. Of these 234 participants, 27 were excluded due to left-handedness; 22 due to poor data quality (excessive head motion; significant signal loss; and partial brain coverage); 36 due to use of psychoactive medication; and 18 for carrying an *ε2* allele. This left us with a total of 131 participants that were included. Of these 131 participants, 43 were *ε4* carriers, of which 4 were ε4 homozygotes (2 male and 2 female) and 39 were ε3/ε4's (24 male and 15 female), and 88 were *ε3* homozygotes (34 male and 54 female), see table 1 for demographics.

Neuropsychololological Assessment

All participants underwent an extensive neuropsychological assessment. For this study we only considered the results of the mini-mental state examination and the neuropsychological tests targeting memory function: the California Verbal Learning Test, both immediate and delayed recall; and the recall of the Benson Complex Figure. Raw test scores were tested for differences between *APOE* genotype, gender, and the interaction between the two using a multivariate analysis of variance, with $p<0.05$.

APOE genotype assessment

APOE single nucleotide polymorphism (SNP) genotyping was carried out by Real Time polymerase chain reaction (PCR), on an Applied Biosystems 7900HT Real Time PCR machine using the Taqman SNP Genotyping Assay for rs429358 and rs7412 with identification numbers C___3084793_20 and C____904973_10, respectively (Applied Biosystems, Foster City, CA). The protocol was followed as outlined in the manufacturer's instructions, and every assay was performed in duplicate. In addition to a standard curve amplification protocol, an allelic discrimination step was added to facilitate the contrast between the two alleles and their respective reporter dyes. Sequence Detection Systems Software version 2.3 was used to analyze the SNP genotyping data.

MRI data acquisition

Functional MRI scanning was performed at the UCSF Neuroscience Imaging Center on a 3 Tesla Siemens Tim Trio scanner using a standard 12-channel head coil. Thirty-six interleaved axial slices (3 mm thick with a gap of 0.6 mm) were imaged parallel to the plane connecting the anterior and posterior commissures using a T2*-weighted echo planar sequence (repetition time (TR): 2000 ms; echo time (TE): 27ms; flip angle (FA): 80°; voxel size: 2.5 × 2.5 × 3.6 mm). The field of view was 230×230mm, and the matrix size was 92×92. All subjects underwent an 8-minute resting state fMRI scan after being instructed only to remain awake with their eyes closed. A volumetric magnetization prepared rapid gradient echo (MPRAGE) MRI sequence was used to obtain a T1- weighted image of the entire brain in saggital slices (repetition time, 2300 ms; echo time, 2.98 ms; inversion time, 900 ms; flip angle, 9 degrees). The images were reconstructed as a 160×240×256 matrix with 1×1×1 mm spatial resolution.

MRI data analysis

Anatomical data analysis—Anatomical data was analyzed with FSL-VBM, a voxel-based morphometry style analysis (Ashburner and Friston, 2000; Good et al., 2001) carried out with FSL tools (Smith et al.). First, anatomical images were brain-extracted using BET (Smith, 2002). Next, tissue-type segmentation was carried out using FAST4 (Zhang et al., 2001). The resulting grey-matter partial volume images were then aligned to MNI152 standard space using the affine registration tool FLIRT (Jenkinson and Smith, 2001; Jenkinson et al., 2002), followed by nonlinear registration using FNIRT (Andersson 2007, FMRIB technical reports TR07JA1 and TR07JA2, available at: www.fmrib.ox.ac.uk/analysis/techrep), which uses a b-spline representation of the registration warp field (Rueckert et al., 1999). For the use of grey matter volume as a voxel-wise regressor in the fMRI data analysis, a 4D image was created by concatenating every individual's standard space grey matter image. For the direct comparison of grey matter volume, the individual standard space grey matter images were averaged to create a study-specific template, to which the native grey matter images were then non-linearly re-registered. The registered partial volume images were then modulated (to correct for local expansion or contraction), by dividing by the Jacobian of the warp field. The modulated segmented images were then smoothed with an isotropic Gaussian kernel with a sigma of 3

mm. Finally, to test for significant differences between *ε4* carriers and *ε3* homozygotes, a voxel-wise general linear model was applied using permutation-based non-parametric testing, using TFCE as implemented in FSL (Smith and Nichols, 2009), and $p<0.05$ family-wise error corrected.

Resting State fMRI data analysis—Image preprocessing was carried out using tools from FMRIB's Software Library (FSL, version 4.1) (Smith et al., 2004). The following pre-statistics processing was applied: motion correction (Jenkinson et al., 2002); removal of non-brain structures (Smith, 2002); spatial smoothing using a Gaussian kernel of 6mm full width at half maximum; mean-based intensity normalization of all volumes by the same factor (i.e. 4D grand-mean scaling in order to ensure comparability between data sets at the group level); high-pass temporal filtering (Gaussian-weighted least-squares straight line fitting, with sigma = 75.0s); and Gaussian low-pass temporal filtering (sigma = 2.8s). After pre-processing the functional scan was first aligned to the individual's high resolution T1-weighted image, which was subsequently registered to the MNI152 standard space (average T1 brain image constructed from 152 normal subjects at Montreal Neurological Institute) using affine linear registration (Jenkinson et al., 2002). To perform voxel-wise between group comparisons of resting state connectivity, the dual regression technique as described in (Filippini et al., 2009; Veer et al., 2010; Damoiseaux et al., 2011) was used. This approach entails three steps: First, creating data-driven population specific spatial maps showing large-scale connectivity patterns, by running group independent component analysis (ICA) on the concatenated resting state data of equal numbers of *ε4* carriers, *ε3* homozygotes, males and females (17 subjects per group; 68 total). Equal numbers of subjects per sub-group were used here to avoid introducing bias in the creation of the connectivity networks of interest. The dataset was decomposed into 30 independent components. Second, performing the actual dual regression by (i) using all the 30 independent components in a linear model fit (spatial regression) against all the 131 individual datasets, resulting in specific time courses for each independent component and subject, and (ii) using these time courses in a linear model fit (temporal regression) against the individual's resting state data to estimate subject-specific spatial maps. Lastly, performing voxel-wise between group statistical testing on the subject-specific spatial maps using nonparametric permutation testing (5000 permutations) (Nichols and Holmes, 2002). To control for differences in grey matter volume, the individual grey matter partial volume maps were included as a voxel-wise regressor in the between-group comparison, as described by (Oakes et al., 2007) and implemented in FSL.

The DMN and a control network in which we did not expect to find any changes (i.e. the primary visual network) were selected for between-group analyses. In line with previous observations (Damoiseaux et al., 2011; Westlye et al., 2011), the default-mode network was divided into three sub-networks (referred to here as the anterior, posterior, and ventral DMNs), identified by visual inspection of the group ICA. In order to assess any potential differences in modulation of these networks, we included all three networks in the analysis plus the primary visual network (identified by visual inspection as a single independent component). See figure 1 for a visual representation of all the networks included in the analyses. The fractionation of the DMN into several sub-networks has been observed in multiple previous studies that either used a different methodology (i.e. seed-based correlations) and/or studied a different population (i.e. younger healthy adults) (Uddin et al., 2009; Andrews-Hanna et al., 2010; Littow et al., 2010; Westlye et al., 2011). In addition, sub-divisions of the default mode system have been associated with distinct cognitive functions (Uddin et al., 2009; Andrews-Hanna et al., 2010; Qin et al., 2011; Whitfield-Gabrieli et al., 2011). We therefore believe that this fractionation is not merely a methodological artifact, but that it represents resting state networks with distinct functional attributes.

To find significant differences between *ε4* carriers and *ε3* homozygotes, a voxel-wise general linear model was applied using permutation-based non-parametric testing, using TFCE with $p<0.05$ family-wise error corrected, spatially masked with the thresholded group ICA component in question (posterior probability threshold of $p>0.5$), and a cluster size greater than 10 voxels. Given our a priori hypothesis and the reduced *n* when splitting by gender, we used TFCE with a more lenient threshold of $p<0.01$ uncorrected, spatially masked with the thresholded group ICA component in question, and a cluster size greater than 10 voxels, for the genotype by gender interaction analysis and subsequent post-hoc comparisons.

ADNI data

Data used in this part of the study were obtained from the ADNI database (adni.loni.ucla.edu). The primary goal of ADNI has been to test whether serial MRI, positron emission tomography (PET), other biological markers, and clinical and neuropsychological assessment can be combined to measure the progression of MCIand early AD. Determination of sensitive and specific markers of very early AD progression is intended to aid researchers and clinicians to develop new treatments and monitor their effectiveness, as well as lessen the time and cost of clinical trials.

ADNI is the result of efforts of many co-investigators from a broad range of academic institutions and private corporations, and subjects have been recruited from over 50 sites across the U.S. and Canada. The initial goal of ADNI was to recruit 800 adults, ages 55 to 90, to participate in the research, approximately 200 cognitively normal older individuals to be followed for 3 years, 400 people with MCI to be followed for 3 years and 200 people with early AD to be followed for 2 years. These initial goals were met and the ADNI project has now been extended as ADNI-2.

Subjects—Within the ADNI database, three separate spreadsheets hold cerebrospinal fluid (CSF) measures; for our analyses we used the original ADNI baseline data from the ‘upennbiomark’ spreadsheet. In this spreadsheet 114 healthy controls have CSF data. Out of these 114 subjects, 21 were *ε2* carriers and therefore excluded from our analyses. The remaining subjects were included in our analysis, out of these 93 subjects, 26 were *ε4* carriers (2 *ε*4 homozygotes, 1 male and 1 female; and 24 *ε*3/*ε*4’s, 16 male and 8 female) and 67 were *ε3* homozygotes (32 male and 35 female) (see table 1 for demographics).

Cerebrospinal fluid analysis—CSF samples were collected at different ADNI sites as described in the ADNI procedures manual (http://www.adni-info.org/). It was then shipped overnight on dry ice to the ADNI Biomarker Core laboratory at the University of Pennsylvania Medical Center. All analyses, as described in Shaw and colleagues (2009), were performed at this location. Mean levels of total tau, amyloid $ß_{1-42}$ ($Aß_{1-42}$), and phosphotau (p-tau), in pg/ml, were tested for differences between *APOE* genotype, gender, and the interaction between the two, using a multivariate analysis of variance, with $p<0.05$. Subsequent post-hoc comparisons were performed using the Mann- Whitney U test (one-tailed).

Results

Demographics

We did not find a significant difference between *APOE* groups in either age or years of education. The distribution of gender across the *APOE* groups did differ (Pearson Chi-Square, $p=0.019$). No interaction between *APOE* genotype and gender was observed for any of these measures. See table 1 for details.

Neuropsychology

No significant between-group differences or *APOE* genotype by gender interactions were found for mini-mental state examination scores or memory performance, as measured with the California Verbal Learning Test, immediate and delayed recall; and the recall of the Benson Complex Figure (see table 1).

APOE ε4 effect on functional connectivity

We first compared functional connectivity within our four networks between all *ε4* carriers and all ε3 homozygotes, while correcting voxel-wise for grey matter volume. We found decreased connectivity in *ε4* carriers compared to ε3 homozygotes in two large frontal clusters of the anterior DMN (see figure 2A, and table 2), and in a posterior cingulate cluster of the posterior DMN (see figure 2B, and table 2), using 'Threshold-Free Cluster Enhancement' (TFCE) and a $p<0.05$ family- wise error correction. No differences were observed in the opposite direction, and no differences were observed in either the ventral DMN or the primary visual network.

To visualize the distribution of the observed effect across genotype and gender, we extracted the mean parameter estimate per group for a significant cluster in each network that showed significant differences between *ε4* carriers and ε3 homozygotes (note: these are the individual values before the grey matter volume correction is applied). For the anterior DMN we selected a representative cluster in the right anterior cingulate gyrus, and for the posterior DMN the left posterior cingulate gyrus. In both clusters the ε4 women have the lowest mean value (see bar graphs in figure 2). The difference across both genotype ($p<0.001$) and gender ($p=0.005$) is significant for the anterior cingulate gyrus. For the posterior cingulate gyrus only the difference across genotype is significant ($p=0.001$).

APOE genotype and gender interaction

We then tested voxel-wise for an *APOE* by gender interaction in the anterior and posterior DMNs, the two networks that showed an *ε4* effect, again correcting voxel-wise for grey matter volume. This analysis revealed a significant interaction in the precuneus, a major hub within the posterior DMN (Hagmann et al., 2008) (see figure 3 and table 3), using TFCE and $p<0.01$ uncorrected. The bar graph in figure 3 shows the distribution across genotype and gender for this region. Not surprisingly the interaction was significant ($p<0.001$), but the main effects of genotype and gender were not. No significant interaction between *APOE* genotype and gender was observed in the anterior DMN. Given the significant interaction in the posterior DMN, post-hoc voxel-wise testing was performed for this network (using TFCE and $p<0.01$ uncorrected) for the following three specific contrasts: female ε3 homozygotes > female ε4 carriers; male ε3 homozygotes > male ε4 carriers; and male ε4 carriers > female ε4 carriers. The results showed the most prominent reduction in posterior default mode functional connectivity in female ε4 carriers compared to female ε3 homozygotes, mainly in a large (>2000 voxel) cluster encompassing the cuneal cortex, precuneus and posterior cingulate gyrus. Male ε4 carriers showed decreased posterior default mode connectivity only in a small (16 voxel) cluster in the left superior parietal cortex compared to male ε3 homozygotes. In addition, female ε4 carriers also showed reduced functional connectivity compared to male ε4 carriers in a cuneus/precuneus cluster of the posterior DMN. See figure 4 and table 3 for specifics of the post-hoc results.

APOE ε4 effect on grey matter volume

We also tested the effect of *ε4* on grey matter volume. No significant between-group differences or *APOE* genotype by gender interactions were found.

ADNI cerebrospinal fluid

In order to obtain convergent evidence for the imaging findings we also tested the same model in an analysis of CSF protein levels in a total of 93 healthy older controls from the ADNI dataset. As with the imaging dataset, we did not find a significant difference between *APOE* groups in either age or years of education and there were no significant interactions between *APOE* genotype and gender for either measure. As has been shown previously (Shaw et al., 2009), we found a difference between *ε4* carriers and *ε*3 homozygotes on all three CSF protein measures, total tau ($p=0.022$), $Aß_{1-42}$ ($p<0.001$), and p-tau ($p=0.020$). In addition, we found a significant *APOE* genotype by gender interaction for CSF total tau levels ($p=0.024$), see figure 5. CSF total tau levels were highest in female *ε4* carriers (mean 99 ± 56 pg/ml) and lowest in female *ε*3 homozygotes (mean 65 ± 21 pg/ml), which was a significant difference ($p=0.046$). The same comparison in the men showed no significant differences between the male *ε4* carriers (mean 72 ± 28 pg/ml) and the male *ε*3 homozygotes (mean 71 ± 32 pg/ml; $p=0.446$). No significant differences were found in the other pairwise contrasts: female vs. male *ε4* carriers ($p=0.144$) and female vs. male *ε*3 homozygotes ($p=0.319$). No significant interaction was observed for either $Aß_{1-42}$ ($p=0.418$) or pTau ($p=0.645$).

Discussion

*APOE ε*4 is a potent AD risk factor. In the normal population 10-15% of people carry the *ε4* allele; among AD patients, up to 65% are *ε4* carriers (Saunders et al., 1993; Farrer et al., 1997). The mechanism through which *ε4* exerts its effect remains elusive, but possibilities include, promotion of tau hyperphosphorylation, reduction of beta-amyloid clearance, and inhibition of neurite outgrowth (Kim et al., 2009). Previous studies of AD risk have shown that the *ε4* effect is more pronounced in females (Payami et al., 1996; Farrer et al., 1997; Bretsky et al., 1999). With notable exceptions (Corder et al., 2004; Fleisher et al., 2005; Lehmann et al., 2006), most studies have ignored this gender effect. No previous studies have investigated whether the interaction between gender and *APOE* is detectable in healthy adults. Here we have shown that this interaction is detectable in healthy older adults using two distinct AD biomarkers in two independent samples.

DMN connectivity is a well-replicated imaging biomarker of AD (Greicius et al., 2004; Buckner et al., 2005; Damoiseaux et al., 2011). Our most compelling imaging results demonstrate an *APOE* genotype by gender interaction on posterior DMN connectivity. The precuneus/cuneus region of the posterior DMN showed a significant interaction, with the greatest reduction of functional connectivity in female *ε4* carriers (Figure 3). Post-hoc testing was most notable for a 2000+ voxel cluster in the posterior cingulate/precuneus showing reduced connectivity in female *ε*4 carriers compared to female *ε*3 homozygotes (Figure 4A, Table 3). The same comparison in males only showed reduced connectivity in *ε4* carriers in a small DMN cluster (Figure 4B, Table 3). The small size and unusual location (not a core DMN region) of this cluster lead us to interpret this finding cautiously and strengthen our hypothesis that the *ε4* effect is mainly driven by female carriers. Comparing female and male *ε*4 carriers revealed a decrease in female *ε*4 carriers in three small but more strategically located DMN clusters (Figure 4C, Table 3). In structural and functional connectivity analyses, the posterior cingulate/precuneus region is consistently found to be a core node in the DMN (Hagmann et al., 2008; Buckner et al., 2009). This region is structurally connected to the medial temporal lobes (Greicius et al., 2009), the initial site of tau pathology in AD (Braak and Braak, 1991). It shows reduced glucose metabolism early in AD and in asymptomatic *ε4* carriers (Minoshima et al., 1995; Reiman et al., 1996). Lastly, this region shows reduced connectivity in AD patients compared to controls (Greicius et al., 2004) and in MCI patients compared to controls (Sorg et al., 2007). Thus, the interaction of

gender and *APOE* status occurs in a core DMN node and in the node most tightly linked to AD.

In the anterior DMN we did not observe an *APOE* genotype by gender interaction. However in the cluster highlighted to depict the directionality of the findings (Figure 2A), we saw additive effects of gender and *APOE* genotype. This indicates that, although there is no *APOE* genotype by gender interaction, the additive effects of decreased connectivity in *ε4* carriers and decreased connectivity in females, renders female *ε*4 carriers most vulnerable to the observed *ε4* effect in this region. The observation of gender differences in resting state functional connectivity, including DMN regions, is consistent with many, but not all (Weissman-Fogel et al., 2010), previous studies on this topic (Liu et al., 2009; Biswal et al., 2010; Allen et al., 2011; Filippi et al., 2012).

Our results may explain the prominent discrepancies in the four previous studies examining the effect of *APOE* genotype on DMN connectivity in healthy older individuals (Sheline et al., 2010; Machulda et al., 2011; Trachtenberg et al., 2011; Westlye et al., 2011). Sheline and colleagues (2010) found increases and decreases in DMN connectivity in *ε*4 carriers, Machulda and colleagues (2011) only found decreases, Westlye and colleagues (2011) only found increases, and Trachtenberg and colleagues (2011) found no differences in the DMN but reported differences in two hippocampal networks. The directionality of our findings is most compatible with Machulda and colleagues (2011), who also showed decreased connectivity in *ε4* carriers. The discrepancy in the findings between our study and the prior four could be due to the different age ranges. The participants in our and Machulda and colleagues' studies were older (mean age around 70 and 78, respectively) than those in the other three studies (mean ages around 61, 63, and 45). Perhaps more importantly, the ratio of males to females varied considerably across the previous studies. In the Sheline study there were 29 female and 9 male *ε*4 carriers, and 43 female and 19 male *ε*3 homozygotes; in the Machulda study gender was matched across *APOE* genotype groups, with 21 females and 35 males in each group; in the Westlye study there were 20 female and 13 male *ε*4 carriers, and 41 female and 21 male *ε*3 homozygotes; and in the Trachtenberg study there were 17 female and 17 male *ε*4 carriers and 10 female and 10 male *ε*3 homozygotes. The discrepancy in findings across these previous studies might therefore be explained by an underlying and unexplored *APOE* genotype by gender interaction.

We used the ADNI CSF dataset to obtain convergent evidence of an *APOE* genotype by gender interaction in an independent cohort with an independent biomarker for AD. We found a main effect of *APOE* on all three markers in the expected direction and an *APOE* genotype by gender interaction in total tau levels, where female *ε*4 carriers had significantly elevated levels compared to female *ε*3 homozygotes while male *ε*4 carriers and male *ε*3 homozygotes had nearly identical levels. To our knowledge this is the first report of an *APOE* genotype by gender interaction in a CSF biomarker of AD. Numerous studies have shown that AD and MCI patients have reduced CSF levels of $A\beta_{1\text{-}42}$ and increased levels of p-tau and total tau (Tarawneh and Holtzman, 2010). Shaw and colleagues have previously examined the ADNI healthy control dataset and noted an *APOE* effect on $A\beta_{1\text{-}42}$ levels (reduced in *ε*4 carriers) and p-tau levels (increased in *ε*4 carriers), but did not find a significant *APOE* effect in total tau levels (Shaw et al., 2009). Our analysis differs in that we excluded *ε2* carriers and examined an *APOE* genotype by gender interaction. It is unclear why the *APOE* genotype by gender interaction was detectable in total tau levels but not in p-tau or $A\beta_{1\text{-}42}$ levels, though this might reflect the temporal progression of biomarkers in AD pathology. It is generally accepted that beta- amyloid pathology precedes tau pathology by many years (Jack et al., 2010; Jack et al., 2011). It is possible that p-tau changes precede total tau changes on the pathological progression to AD. This is consistent with the findings in Shaw et al., where healthy *ε4* carriers, collapsed across gender, differ from non-*ε*4

carriers in $A\beta_{1-42}$ levels and p-tau levels but not (yet) in total tau levels. In our analysis, female $\varepsilon 4$ carriers, presumably further along in their AD pathology, show changes in $A\beta_{1-42}$ levels, p-tau levels, and total tau levels whereas male $\varepsilon 4$ carriers only manifest differences in the first two markers.

No differences or *APOE* genotype by gender interactions were observed for grey matter volume or memory performance. Changes in DMN functional connectivity and CSF tau protein levels seem to precede changes in brain structure and cognitive performance. This discrepancy suggests that resting-state functional connectivity and CSF protein analyses may therefore be more sensitive than cognitive testing or structural MRI measures as markers of preclinical AD.

Although we show that female $\varepsilon 4$ carriers have decreased DMN connectivity and increased CSF tau levels, we can only speculate as to the mechanism(s) behind this interaction. The most obvious possibility would be some interaction between *APOE* status and sex hormone levels. Hundreds of studies in animals and humans have examined the effect of estrogen loss and replacement on cognition and dementia risk in older women (see (Henderson, 2009) for a recent review). The negative outcome of the Women's Health Initiative Memory Study, which showed an increased dementia risk in women on estrogen replacement therapy, has only added to the uncertainty regarding estrogen replacement (Shumaker et al., 2004). Regarding our findings, it is notable that the few studies of estrogen and cognition that have stratified by *APOE* status suggest that *APOE* status may be critical in evaluating estrogen replacement (Yaffe et al., 2000; Kang and Grodstein, 2010).

We have demonstrated that gender influences the effect of *APOE* genotype on both DMN connectivity and CSF tau levels, and determined that the detrimental effect of the $\varepsilon 4$ allele is most pronounced in females. Our results support previous work showing a higher prevalence of the $\varepsilon 4$ allele among women with AD and, more critically, demonstrate that this interaction between *APOE* genotype and gender is detectable in the preclinical period. Future studies using biomarkers in the preclinical stages of disease should allow us to dissect the environmental, hormonal, and genetic factors that underlie this interaction which appears central to AD pathogenesis.

Acknowledgments

The authors thank William Irwin, Maria Molfino, and Heidi Jiang for their help with MRI data transfer and preprocessing, and Eric Klein for his help with the *APOE* genotyping. This work was supported by the Hillblom Foundation, the John Douglas French Alzheimer's Disease Foundation, the JNA Foundation, and the following grants from the National Institutes of Health: NS073498 and AG032306.

Alzheimer's Disease Neuroimaging Initiative (ADNI) data: Data collection and sharing for this project was funded by the Alzheimer's Disease Neuroimaging Initiative (ADNI) (National Institutes of Health Grant U01 AG024904). ADNI is funded by the National Institute on Aging, the National Institute of Biomedical Imaging an Bioengineering, and through generous contributions from the following: Abbott; Alzheimer's Association; Alzheimer's Drug Discovery Foundation; Amorfix Life Sciences Ltd.; AstraZeneca; Bayer HealthCare; BioClinica, Inc.; Biogen Idec Inc.; Bristol-Myers Squibb Company; Eisai Inc.; Elan Pharmaceuticals Inc.; Eli Lilly and Company; F. Hoffmann-La Roche Ltd and its affiliated company Genentech, Inc.; GE Healthcare; Innogenetics, N.V.; Janssen Alzheimer Immunotherapy Research & Development, LLC.; Johnson & Johnson Pharmaceutical Research & Development LLC.; Medpace, Inc.; Merck & Co., Inc.; Meso Scale Diagnostics, LLC.; Novartis Pharmaceuticals Corporation; Pfizer Inc.; Servier; Synarc Inc.; and Takeda Pharmaceutical Company. The Canadian Institutes of Health Research is providing funds to support ADNI clinical sites in Canada. Private sector contributions are facilitated by the Foundation for the National Institutes of Health (www.fnih.org). The grantee organization is the Northern California Institute for Research and Education, and the study is coordinated by the Alzheimer's Disease Cooperative Study at the University of California, San Diego. ADNI data are disseminated by the Laboratory for Neuro Imaging at the University of California, Los Angeles.

References

Allen EA, et al. A baseline for the multivariate comparison of resting-state networks. Front Syst Neurosci. 2011; 5:2. [PubMed: 21442040]

Andrews-Hanna JR, Reidler JS, Sepulcre J, Poulin R, Buckner RL. Functional-anatomic fractionation of the brain's default network. Neuron. 2010; 65:550–562. [PubMed: 20188659]

Ashburner J, Friston KJ. Voxel-based morphometry--the methods. Neuroimage. 2000; 11:805–821. [PubMed: 10860804]

Bai F, Watson DR, Shi Y, Wang Y, Yue C, Yuhuan Teng, Wu D, Yuan Y, Zhang Z. Specifically progressive deficits of brain functional marker in amnestic type mild cognitive impairment. PLoS ONE. 2011; 6:e24271. [PubMed: 21935394]

Biswal BB, et al. Toward discovery science of human brain function. Proc Natl Acad Sci U S A. 2010; 107:4734–4739. [PubMed: 20176931]

Braak H, Braak E. Neuropathological stageing of Alzheimer-related changes. Acta Neuropathol. 1991; 82:239–259. [PubMed: 1759558]

Bretsky PM, Buckwalter JG, Seeman TE, Miller CA, Poirier J, Schellenberg GD, Finch CE, Henderson VW. Evidence for an interaction between apolipoprotein E genotype, gender, and Alzheimer disease. Alzheimer Dis Assoc Disord. 1999; 13:216–221. [PubMed: 10609670]

Buckner RL, Sepulcre J, Talukdar T, Krienen FM, Liu H, Hedden T, Andrews-Hanna JR, Sperling RA, Johnson KA. Cortical hubs revealed by intrinsic functional connectivity: mapping, assessment of stability, and relation to Alzheimer's disease. J Neurosci. 2009; 29:1860–1873. [PubMed: 19211893]

Buckner RL, Snyder AZ, Shannon BJ, LaRossa G, Sachs R, Fotenos AF, Sheline YI, Klunk WE, Mathis CA, Morris JC, Mintun MA. Molecular, structural, and functional characterization of Alzheimer's disease: evidence for a relationship between default activity, amyloid, and memory. J Neurosci. 2005:7709–7717. [PubMed: 16120771]

Corder EH, Ghebremedhin E, Taylor MG, Thal DR, Ohm TG, Braak H. The biphasic relationship between regional brain senile plaque and neurofibrillary tangle distributions: modification by age, sex, and APOE polymorphism. Ann N Y Acad Sci. 2004; 1019:24–28. [PubMed: 15246987]

Damoiseaux JS, Prater KE, Miller BL, Greicius MD. Functional connectivity tracks clinical deterioration in Alzheimer's disease. Neurobiol Aging. 2011

Farrer LA, Cupples LA, Haines JL, Hyman B, Kukull WA, Mayeux R, Myers RH, Pericak-Vance MA, Risch N, van Duijn CM, APOE and Alzheimer Disease Meta Analysis Consortium. Effects of age, sex, and ethnicity on the association between apolipoprotein E genotype and Alzheimer disease. A meta-analysis. JAMA. 1997; 278:1349–1356. [PubMed: 9343467]

Filippi M, Valsasina P, Misci P, Falini A, Comi G, Rocca MA. The organization of intrinsic brain activity differs between genders: A resting-state fMRI study in a large cohort of young healthy subjects. Hum Brain Mapp. 2012

Filippini N, MacIntosh BJ, Hough MG, Goodwin GM, Frisoni GB, Smith SM, Matthews PM, Beckmann CF, Mackay CE. Distinct patterns of brain activity in young carriers of the APOE-epsilon4 allele. Proc Natl Acad Sci U S A. 2009; 106:7209–7214. [PubMed: 19357304]

Fleisher A, Grundman M, Jack CR Jr. Petersen RC, Taylor C, Kim HT, Schiller DH, Bagwell V, Sencakova D, Weiner MF, DeCarli C, DeKosky ST, van Dyck CH, Thal LJ. Sex, apolipoprotein E epsilon 4 status, and hippocampal volume in mild cognitive impairment. Arch Neurol. 2005; 62:953–957. [PubMed: 15956166]

Good CD, Johnsrude IS, Ashburner J, Henson RN, Friston KJ, Frackowiak RS. A voxel-based morphometric study of ageing in 465 normal adult human brains. Neuroimage. 2001; 14:21–36. [PubMed: 11525331]

Greicius M, Supekar K, Menon V, Dougherty R. Resting-state functional connectivity reflects structural connectivity in the default mode network. Cereb Cortex. 2009; 19:72–78. [PubMed: 18403396]

Greicius MD, Srivastava G, Reiss AL, Menon V. Default-mode network activity distinguishes Alzheimer's disease from healthy aging: evidence from functional MRI. Proc Natl Acad Sci USA. 2004; 101:4637–4642. [PubMed: 15070770]

Hagmann P, Cammoun L, Gigandet X, Meuli R, Honey C, Wedeen V, Sporns O. Mapping the structural core of human cerebral cortex. PLoS Biol. 2008; 6:e159. [PubMed: 18597554]

Henderson VW. Aging, estrogens, and episodic memory in women. Cogn Behav Neurol. 2009; 22:205–214. [PubMed: 19996872]

Jack CR Jr. Knopman DS, Jagust WJ, Shaw LM, Aisen PS, Weiner MW, Petersen RC, Trojanowski JQ. Hypothetical model of dynamic biomarkers of the Alzheimer's pathological cascade. Lancet Neurol. 2010; 9:119–128. [PubMed: 20083042]

Jack CR Jr. Vemuri P, Wiste HJ, Weigand SD, Aisen PS, Trojanowski JQ, Shaw LM, Bernstein MA, Petersen RC, Weiner MW, Knopman DS. Evidence for ordering of Alzheimer disease biomarkers. Arch Neurol. 2011; 68:1526–1535. [PubMed: 21825215]

Jenkinson M, Smith S. A global optimisation method for robust affine registration of brain images. MedImage Anal. 2001; 5:143–156.

Jenkinson M, Bannister P, Brady M, Smith S. Improved optimization for the robust and accurate linear registration and motion correction of brain images. NeuroImage. 2002; 17:825–841. [PubMed: 12377157]

Kang JH, Grodstein F. Postmenopausal hormone therapy, timing of initiation, APOE and cognitive decline. Neurobiol Aging. 2010

Kim J, Basak JM, Holtzman DM. The role of apolipoprotein E in Alzheimer's disease. Neuron. 2009; 63:287–303. [PubMed: 19679070]

Lehmann DJ, Refsum H, Nurk E, Warden DR, Tell GS, Vollset SE, Engedal K, Nygaard HA, Smith AD. Apolipoprotein E epsilon4 and impaired episodic memory in community-dwelling elderly people: a marked sex difference. The Hordaland Health Study. J Neurol Neurosurg Psychiatry. 2006; 77:902–908. [PubMed: 16595618]

Littow H, Elseoud AA, Haapea M, Isohanni M, Moilanen I, Mankinen K, Nikkinen J, Rahko J, Rantala H, Remes J, Starck T, Tervonen O, Veijola J, Beckmann C, Kiviniemi VJ. Age-Related Differences in Functional Nodes of the Brain Cortex - A High Model Order Group ICA Study. Front Syst Neurosci 4. 2010

Liu H, Stufflebeam SM, Sepulcre J, Hedden T, Buckner RL. Evidence from intrinsic activity that asymmetry of the human brain is controlled by multiple factors. Proc Natl Acad Sci U S A. 2009; 106:20499–20503. [PubMed: 19918055]

Machulda MM, Jones DT, Vemuri P, McDade E, Avula R, Przybelski S, Boeve BF, Knopman DS, Petersen RC, Jack CR Jr. Effect of APOE {varepsilon}4 Status on Intrinsic Network Connectivity in Cognitively Normal Elderly Subjects. Arch Neurol. 2011; 68:1131–1136. [PubMed: 21555604]

Minoshima S, Frey KA, Koeppe RA, Foster NL, Kuhl DE. A diagnostic approach in Alzheimer's disease using three-dimensional stereotactic surface projections of fluorine-18-FDG PET. J Nucl Med. 1995; 36:1238–1248. [PubMed: 7790950]

Nichols TE, Holmes AP. Nonparametric permutation tests for functional neuroimaging: a primer with examples. Hum Brain Mapp. 2002; 15:1–25. [PubMed: 11747097]

Oakes TR, Fox AS, Johnstone T, Chung MK, Kalin N, Davidson RJ. Integrating VBM into the General Linear Model with voxelwise anatomical covariates. NeuroImage. 2007; 34:500–508. [PubMed: 17113790]

Payami H, Zareparsi S, Montee KR, Sexton GJ, Kaye JA, Bird TD, Yu CE, Wijsman EM, Heston LL, Litt M, Schellenberg GD. Gender difference in apolipoprotein E-associated risk for familial Alzheimer disease: a possible clue to the higher incidence of Alzheimer disease in women. Am J Hum Genet. 1996; 58:803–811. [PubMed: 8644745]

Qin P, Liu Y, Shi J, Wang Y, Duncan N, Gong Q, Weng X, Northoff G. Dissociation between anterior and posterior cortical regions during self-specificity and familiarity: A combined fMRI-meta-analytic study. Hum Brain Mapp. 2011

Reiman EM, Caselli RJ, Yun LS, Chen K, Bandy D, Minoshima S, Thibodeau SN, Osborne D. Preclinical evidence of Alzheimer's disease in persons homozygous for the epsilon 4 allele for apolipoprotein E. N Engl J Med. 1996; 334:752–758. [PubMed: 8592548]

Rueckert D, Sonoda LI, Hayes C, Hill DL, Leach MO, Hawkes DJ. Nonrigid registration using free-form deformations: application to breast MR images. IEEE TransMedImaging. 1999; 18:712–721.

Saunders AM, Strittmatter WJ, Schmechel D, George-Hyslop PH, Pericak-Vance MA, Joo SH, Rosi BL, Gusella JF, Crapper-MacLachlan DR, Alberts MJ, et al. Association of apolipoprotein E allele epsilon 4 with late-onset familial and sporadic Alzheimer's disease. Neurology. 1993; 43:1467–1472. [PubMed: 8350998]

Scott WK, Saunders AM, Gaskell PC, Locke PA, Growdon JH, Farrer LA, Auerbach SA, Roses AD, Haines JL, Pericak-Vance MA. Apolipoprotein E epsilon2 does not increase risk of early-onset sporadic Alzheimer's disease. Ann Neurol. 1997; 42:376–378. [PubMed: 9307262]

Shaw LM, Vanderstichele H, Knapik-Czajka M, Clark CM, Aisen PS, Petersen RC, Blennow K, Soares H, Simon A, Lewczuk P, Dean R, Siemers E, Potter W, Lee VM, Trojanowski JQ. Cerebrospinal fluid biomarker signature in Alzheimer's disease neuroimaging initiative subjects. Ann Neurol. 2009; 65:403–413. [PubMed: 19296504]

Sheline YI, Morris JC, Snyder AZ, Price JL, Yan Z, D'Angelo G, Liu C, Dixit S, Benzinger T, Fagan A, Goate A, Mintun MA. APOE4 allele disrupts resting state fMRI connectivity in the absence of amyloid plaques or decreased CSF Abeta42. J Neurosci. 2010; 30:17035–17040. [PubMed: 21159973]

Shumaker SA, Legault C, Kuller L, Rapp SR, Thal L, Lane DS, Fillit H, Stefanick ML, Hendrix SL, Lewis CE, Masaki K, Coker LH. Conjugated equine estrogens and incidence of probable dementia and mild cognitive impairment in postmenopausal women: Women's Health Initiative Memory Study. JAMA. 2004; 291:2947–2958. [PubMed: 15213206]

Smith SM. Fast robust automated brain extraction. HumBrain Mapp. 2002; 17:143–155.

Smith SM, Nichols TE. Threshold-free cluster enhancement: addressing problems of smoothing, threshold dependence and localisation in cluster inference. NeuroImage. 2009; 44:83–98. [PubMed: 18501637]

Smith SM, Jenkinson M, Woolrich MW, Beckmann CF, Behrens TE, Johansen-Berg H, Bannister PR, De Luca M, Drobnjak I, Flitney DE, Niazy RK, Saunders J, Vickers J, Zhang Y, De Stefano N, Brady JM, Matthews PM. Advances in functional and structural MR image analysis and implementation as FSL. NeuroImage. 2004; 23(Suppl 1):S208–S219. [PubMed: 15501092]

Sorg C, Riedl V, Mühlau M, Calhoun V, Eichele T, Läer L, Drzezga A, Förstl H, Kurz A, Zimmer C, Wohlschläger A. Selective changes of resting-state networks in individuals at risk for Alzheimer's disease. Proc Natl Acad Sci U S A. 2007; 104:18760–18765. [PubMed: 18003904]

Strittmatter WJ, Saunders AM, Schmechel D, Pericak-Vance M, Enghild J, Salvesen GS, Roses AD. Apolipoprotein E: high-avidity binding to beta-amyloid and increased frequency of type 4 allele in late-onset familial Alzheimer disease. Proc Natl Acad Sci U S A. 1993; 90:1977–1981. [PubMed: 8446617]

Tarawneh R, Holtzman DM. Biomarkers in translational research of Alzheimer's disease. Neuropharmacology. 2010; 59:310–322. [PubMed: 20394760]

Trachtenberg AJ, Filippini N, Ebmeier KP, Smith SM, Karpe F, Mackay CE. The effects of APOE on the functional architecture of the resting brain. NeuroImage. 2011; 59:565–572. [PubMed: 21851856]

Uddin LQ, Kelly AM, Biswal BB, Xavier Castellanos F, Milham MP. Functional connectivity of default mode network components: correlation, anticorrelation, and causality. Hum Brain Mapp. 2009; 30:625–637. [PubMed: 18219617]

Veer IM, Beckmann CF, van Tol MJ, Ferrarini L, Milles J, Veltman DJ, Aleman A, van Buchem MA, van der Wee NJ, Rombouts SA. Whole brain resting-state analysis reveals decreased functional connectivity in major depression. Front Syst Neurosci 4. 2010

Wang K, Liang M, Wang L, Tian L, Zhang X, Li K, Jiang T. Altered functional connectivity in early Alzheimer's disease: a resting-state fMRI study. Hum Brain Mapp. 2007; 28:967–978. [PubMed: 17133390]

Weissman-Fogel I, Moayedi M, Taylor KS, Pope G, Davis KD. Cognitive and default-mode resting state networks: do male and female brains "rest" differently? Hum Brain Mapp. 2010; 31:1713–1726. [PubMed: 20725910]

Westlye ET, Lundervold A, Rootwelt H, Lundervold AJ, Westlye LT. Increased hippocampal default mode synchronization during rest in middle-aged and elderly APOE epsilon4 carriers: relationships with memory performance. J Neurosci. 2011; 31:7775–7783. [PubMed: 21613490]

Whitfield-Gabrieli S, Moran JM, Nieto-Castanon A, Triantafyllou C, Saxe R, Gabrieli JD. Associations and dissociations between default and self-reference networks in the human brain. NeuroImage. 2011; 55:225–232. [PubMed: 21111832]

Yaffe K, Haan M, Byers A, Tangen C, Kuller L. Estrogen use, APOE, and cognitive decline: evidence of gene-environment interaction. Neurology. 2000; 54:1949–1954. [PubMed: 10822435]

Zhang HY, Wang SJ, Xing J, Liu B, Ma ZL, Yang M, Zhang ZJ, Teng GJ. Detection of PCC functional connectivity characteristics in resting-state fMRI in mild Alzheimer's disease. Behav Brain Res. 2009; 197:103–108. [PubMed: 18786570]

Zhang Y, Brady M, Smith S. Segmentation of brain MR images through a hidden Markov random field model and the expectation-maximization algorithm. IEEE TransMedImaging. 2001; 20:45–57.

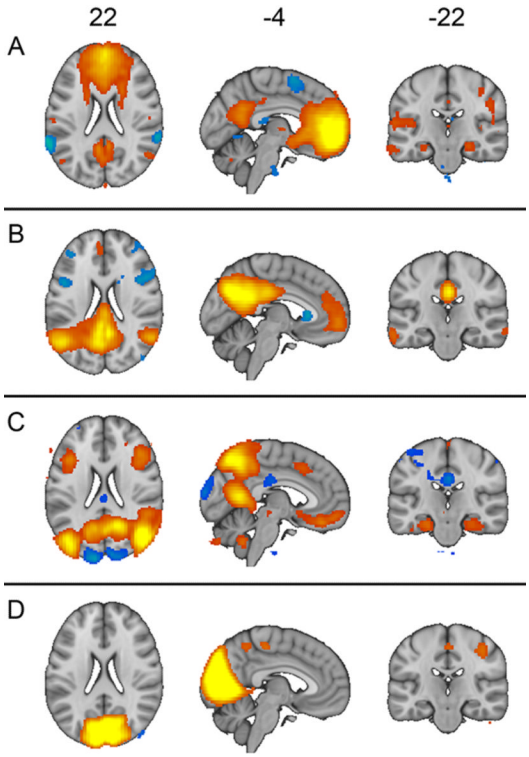

Figure 1.

Spatial maps of the networks of interest and the control network.

The group independent components selected for between-group statistics include three networks of interest: (A) anterior; (B) posterior; and (C) ventral DMN; and (D) the primary visual network as a control. Shown here using a posterior probability threshold of $p>0.5$; MNI coordinates (in mm) of the axial, sagittal and coronal slices are show at the top. Images are displayed in neurological convention.

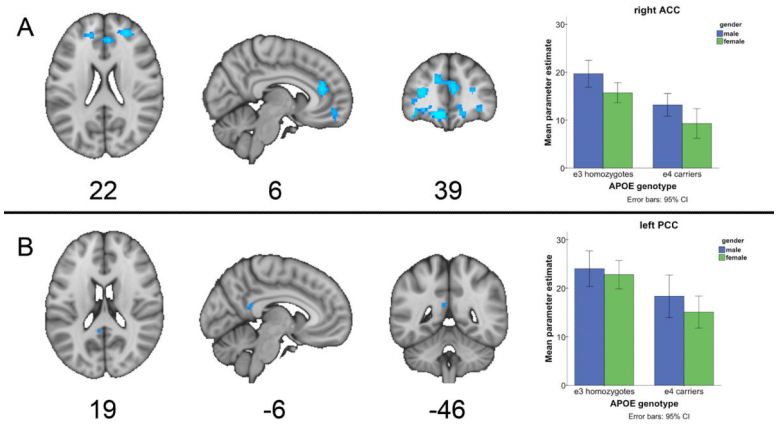

Figure 2.

APOE ε4 reduces default mode connectivity in healthy older adults.

Functional connectivity is decreased in ε4 carriers compared to ε3 homozygotes in both the A) anterior, and (B) posterior DMN. The bar graphs depict the distribution of the effects across sub-groups. They show the mean parameter estimates of a selected region within the anterior DMN (the right anterior cingulate gyrus) and the left posterior cingulate cluster within the posterior DMN, for male and female ε3 homozygotes and male and female ε4 carriers. The difference across both genotype ($p<0.001$) and gender ($p=0.005$) is significant for the anterior cingulate gyrus. For the posterior cingulate gyrus only the difference across genotype is significant ($p=0.001$). The statistical maps, thresholded using TFCE and $p<0.05$ family wise error corrected, are overlaid on the MNI152 brain; MNI coordinates (in mm) of the slices are displayed. Images are displayed in neurological convention.

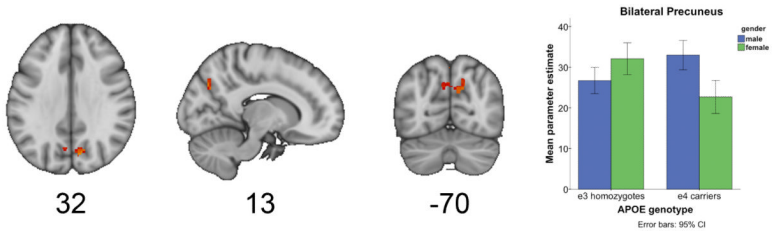

Figure 3.

Gender modulates the *APOE* effect on default mode connectivity.

An *APOE* genotype by gender interaction was found in a precuneus/cuneus region within the posterior DMN. The bar graph shows the mean parameter estimates of this cluster, for male and female *ε*3 homozygotes and male and female *ε*4 carriers. The greatest reduction in functional connectivity was observed in the female *ε*4 carriers. The statistical maps, thresholded using TFCE and $p<0.01$ uncorrected, are overlaid on the MNI152 brain; MNI coordinates (in mm) of the slices are displayed. Images are displayed in neurological convention.

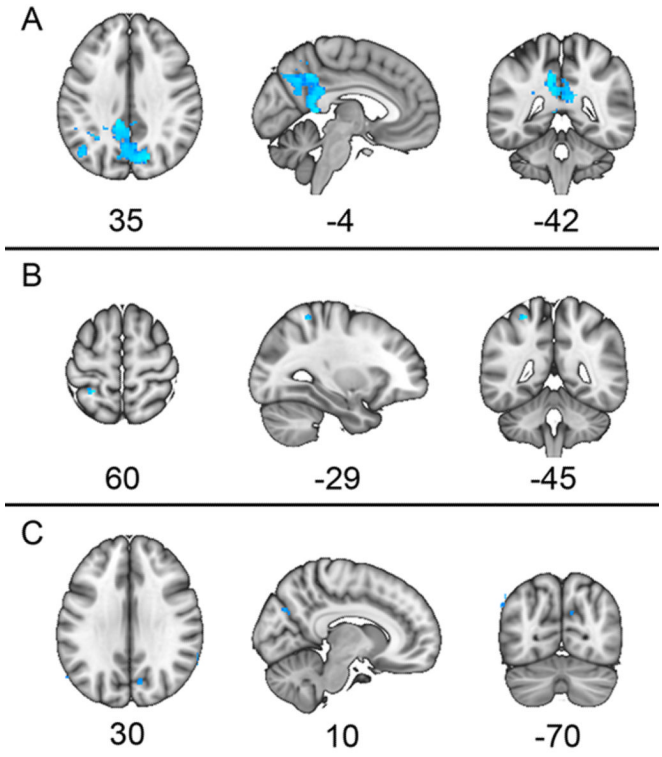

Figure 4.

The *APOE* effect on functional connectivity is most prominent in female ε4 carriers. Post-hoc tests were performed for the posterior DMN for three contrasts: (A) female ε3 homozygotes > female ε4 carriers, which showed a decrease in functional connectivity in female ε4 carriers, mainly in a large (>2000 voxel) cluster encompassing the cuneal cortex, precuneus and posterior cingulate gyrus; (B) male ε3 homozygotes > male ε4 carriers, which showed decreased posterior default mode connectivity in male ε4 carriers in a small (16 voxel) cluster in the left superior parietal cortex; and (C) male ε4 carriers > female ε4 carriers, which showed small clusters of reduced functional connectivity in female ε4 carriers. The statistical maps, thresholded using TFCE and $p<0.01$ uncorrected, are overlaid on the MNI152 brain; MNI coordinates (in mm) of the slices are displayed. Images are displayed in neurological convention.

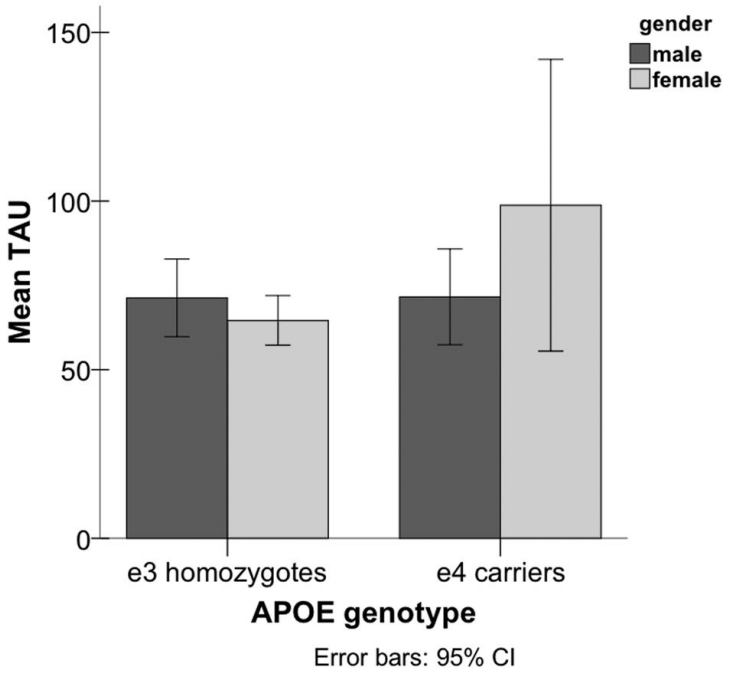

Figure 5.

Cerebrospinal fluid total tau levels provide convergent evidence for the modulation of the *APOE* effect by gender.

The bar graph shows the significant *APOE* genotype by gender interaction observed for CSF total tau levels (p=0.024), in the healthy older controls of the ADNI dataset. Healthy female $\varepsilon 4$ carriers showed the highest mean total tau level. Post-hoc testing revealed a significant difference between female $\varepsilon 4$ carriers and female $\varepsilon 3$ homozygotes (p=0.046).

Table 1

demographics and neuropsychological measures

		ε3 homozygotes	ε4 carriers	ε3 homozygotes vs. ε4 carriers (*P*)	*APOE* x gender interaction (*P*)
Imaging dataset	Gender (m/f)	34/54	26/17	0.019 * (Pearson	-
	Age	70.8 ± 6.9	70.2 ± 6.9	0.659	0.413
	Education (years) *	17.5 ± 2.1	17.0 ± 2.6	0.240	0.917
	MMSE	29.3 ± 0.9	29.2 ± 1.0	0.490	0.754
	CVLT immediate recall	11.1 ± 2.8	10.8 ± 3.5	0.879	0.329
	CVLT delayed recall	11.7 ± 3.1	11.8 ± 3.3	0.622	0.315
	Benson Complex Figure recall	11.4 ± 2.5	11.3 ± 2.4	0.934	0.639
ADNI dataset	Gender (m/f)	32/35	17/9	0.127 (Pearson Chi-Square)	-
	Age	75.9 ± 5.0	75.9 ± 5.8	0.919	0.723
	Education (years) *	16.1 ± 2.5	15.6 ± 3.1	0.269	0.358
	MMSE	29.2 ± 1.0	29.1 ± 0.8	0.815	0.432

MMSE: mini mental state examination; CVLT: California Verbal Learning Test

* significant at $p<0.05$

Table 2

Brain clusters showing significant differences between *APOE* ε3 homozygotes and ε4 carriers.

				Peak MNI coordinates (mm)		
Brain Network	**Contrast**	**Brain region**	**Cluster size (voxels)**	**X**	**Y**	**Z**
Anterior DMN	ε3 homozygotes > ε4 carriers	*RH* Frontal Pole/ Anterior Cingulate/ Medial Prefronta	1435	26	46	24
		Medial Prefrontal *LH* Frontal Pole/ Medial Prefrontal	945	−30	44	−10
Posterior DMN	ε3 homozygotes > ε4 carriers	*LH* Posterior Cingulate Gyrus	17	−6	−48	18

DMN: default mode network; LH: Left Hemisphere; RH: Right Hemisphere

Table 3

Brain clusters showing an interaction between APOE genotype and gender, and clusters showing differences in subsequent post-hoc comparisons.

				Peak MNI coordinates (mm)		
Brain Network	**Contrast**	**Brain region**	**Cluster size (voxels)**	**X**	**Y**	**Z**
Posterior DMN	*APOE* x gender interaction	*RH* Cuneal Cortex/ Precuneus	73	12	−72	32
			49	0	−70	38
Posterior DMN	Female ε3 homozygotes > female ε4 carriers	RH Cuneal Cortex/ Precuneus/ Posterior Cingulate Cortex	2193	18	−74	32
		LH Lateral Occipital Cortex	52	−44	−64	16
		LH Supramarginal Gyrus	36	−50	−46	42
		LH Middle Frontal Gyrus	13	−38	12	50
Posterior DMN	Male ε3 homozygotes > male ε4 carriers	LH Superior Parietal Lobule	16	−28	−48	60
Posterior DMN	Male ε4 carriers > female ε4 carriers	RH Angular Gyrus	85	62	−50	40
		LH Lateral Occipital Cortex	30	−52	−74	40
		RH Cuneal Cortex/ Precuneus	21	12	−74	32

DMN: default mode network; LH: Left Hemisphere; RH: Right Hemisphere